World Journal of Nano Science and Engineering, 2011, 1, 129-136
doi:10.4236/wjnse.2011.14019 Published Online December 2011 (http://www.SciRP.org/journal/wjnse)

A Highly Efficient and Stable Visible-Light Plasmonic Photocatalyst Ag-AgCl/CeO_2

Hongjuan Wang, Lin Yang, Hao Yu, Feng Peng*
The School of Chemistry and Chemical Engineering, South China University of Technology, Guangzhou, China
*E-mail: *cefpeng@scut.edu.cn*
Received September 15, 2011; *revised September* 27, 2011; *accepted October* 29, 2011

Abstract

Noble metal Ag nanoparticles with unique surface plasmon resonance property have attracted much attention recently in the field of photocatalysis. Based on the advantages of Ag nanoparticles and semiconductor CeO_2, a novel plasmonic photocatalyst Ag-AgCl/CeO_2 was prepared with a facile route. The as-prepared samples were characterized using scanning and transmission electron microscopy, X-ray photoelectron spectroscopy and UV-vis diffusion reflection spectroscopy. This metal-semiconductor nanocomposite plasmonic photocatalyst exhibited a high visible-light photocatalytic activity and good stability for photocatalytic degradation of methyl orange in water. Ag-AgCl/CeO_2 will be a potentially promising plasmonic photocatalysts for organic pollutant degradation and water purification.

Keywords: Plasmonic Photocatalyst, Ag Nanoparticle, AgCl, Visible Light, Photocatalytic Degradation

1. Introduction

Due to its high efficiency, low cost and availability, TiO_2 has appeared as a leading photocatalyst candidate since 1970s [1]. However, TiO_2 can only absorb UV light due to its high band gap energy and then cause its low efficient utilization of solar energy [2-7]. During the last decade, a considerable number of new photocatalytic materials have been proposed as potential substitutes of TiO_2 [8]. CeO_2, as an n-type semiconductor, is one of them. With a band-gap of 2.9 - 3.2 eV, it has some properties like titania, such as nontoxicity and high stability [9,10]. So far, CeO_2 are mainly applied in solid oxide fuel cells, oxygen gas sensors, fluorescent materials, metal oxide semiconductor devices, and three way catalysts in vehicle emission control systems and ultraviolet blocking materials, etc. [11-13]. As a potential photocatalyst for the oxidation of pollutants, CeO_2 is less active than TiO_2 under UV irradiation [14-16]. But it can be activated by visible light [8].

Noble-metal nanoparticles (NPs) can give strong visiblelight absorption because of their size- and shape-dependent plasmon resonance [17]. In particular, Ag NPs show efficient surface plasmon resonance (SPR), which can dramatically enhance the photocatalysts' absorption in the visible region [18,19]. This character has been utilized to develop a plasmonic photocatalyst, which has become a hotspot in the field of photocatalyst in recent years. In some researchers' work, noble metal nanoparti= cles were doped in semi-conductors or combined with other non-photoelectric response materials to increase their photocatalytic performance under visible light. In Awazu's report [18], Ag/SiO_2/TiO_2 plasmonic photocatalyst was constructed with Ag NPs as core and the silica as shell to prevent oxidation of Ag by direct contact with TiO_2. The results showed that the degradation rate of methylene blue (MB) was greatly boosted by the assistance of the SPR effect of the contacted silver nanoparticles under near-UV irradiation. Sun *et al*. [20] demonstrated that Ag@C core/shell nanocomposite synthesized by a hydrothermal process was photoactive in destroying aqueous tetraethylated rhodamine (RhB) and gaseous acetaldehyde (CH_3CHO) under visible-light irradiation. Besides using Ag NPs, silver halides were also used in the plasmonic photocatalyst [21]. Wang *et al*. [22-25] utilized the silver halides to develop Ag@AgX plasmonic photocatalysts with high activity and stability under visible light. The improved photocatalytic activity of the silver halides was attributed to the plasmon resonance of Ag NPs from Ag halides reduced on the surface under irradiation [26]. Hu *et al*. [27-29] prepared Ag-AgBr/TiO_2, Ag/AgBr/Al_2O_3 and Ag/AgI/Al_2O_3 plasmonic photocatalyst by deposition-precipitation and photor-eduction method to destruct azodyes and bacteria under visible light. On

the basis of electron spin resonance and cyclic voltammetry analysis, plasmon-induced photocatalytic mechanism was proposed, in which there were two electron transfer processes. O_2^- and excited h^+ on Ag NPs, as the main active species, were involved in the photoreaction system of $Ag/AgI/Al_2O_3$ and $Ag/AgBr/Al_2O_3$.

In this work, based on the advantages of Ag, silver halides and semiconductor CeO_2, a novel plasmonic photocatalyst $Ag\text{-}AgCl/CeO_2$ was designed and prepared. The results showed that the synthesized catalysts had higher photoactivity and stability, showing the potential of $Ag\text{-}AgCl/CeO_2$ as a promising photocatalytic material for organic pollutant degradation under visible light.

2. Experimental Section

2.1. Preparation of the Catalysts

All the chemicals used were analytical grade and used without further purification. CeO_2 was purchased from Rare Chemical Corporation of China. To prepare the $AgCl/CeO_2$, the deposition-precipitation method was adopted. In a typical experiment, 1 g CeO_2 was added into 100 mL deionized water and sonicated for 30 min to form a suspension, followed by the addition of 0.1 g $AgNO_3$ and kept stirring for 30 min. Then 1 M HCl solution was added, and kept stirring for another 60 min. After that, the resulting suspension was centrifuged and washed with deionized water until pH = 7. The obtained solid paste was dried at around 90˚C overnight to obtain $AgCl/CeO_2$.

$Ag\text{-}AgCl/CeO_2$ was prepared via a photo-reduction method. A suspension of $AgCl/CeO_2$ in deionized water was formed by sonication for 15 min, and then irradiated with a 300 W Hg lamp for 20 min to reduce some Ag^+ to Ag. The resulting product with some silver NPs deposited on $AgCl/CeO_2$ was washed and dried in the air to obtain $Ag\text{-}AgCl/CeO_2$.

For comparison, Ag/CeO_2 with the same Ag content as that of $Ag\text{-}AgCl/CeO_2$ was also prepared with incipient wetness impregnation method at room temperature. The samples were dried at 120˚C for 2 h, calcined in air at 600˚C for 6 h and then reduced in a flow of H_2/N_2 (20 vol% H_2, 50 $mL{\cdot}min^{-1}$) at 400˚C for 2 h. As reference, Ag-AgCl sample was prepared via photo-reduction method according to the same method as $Ag\text{-}AgCl/CeO_2$.

2.2. Characterization of the Catalysts

The morphology characterization of the samples was performed on a scanning electron microscope (SEM, LEO1530VP), transmission electron microscopy (TEM, JEOL JEM 2010) using a 200 kV accelerating voltage. The crystal structures of the samples were examined by XRD (D/max-IIIA, Japan) using Cu Kα as the radiation source. UV-Vis diffuse reflection absorption spectra (UV-Vis/DRS) of the samples were recorded by an UV-Vis spectrometer (U3010, Hitachi) equipped with an integrating sphere accessory in the diffuse reflectance mode (R) and $BaSO_4$ as a reference material. The chemical valences of Ag in the samples were analyzed by X-ray photoelectron spectroscopy (XPS, VG Scientific, ESCALAB MKII) using Al Kα radiation (1486.71 eV). Spectra correction was conducted by using a C 1s binding energy of 284.6 eV. The BET surface areas of the samples were measured by N_2 adsorption at 77 K using a TriStar 3000 (Micromeritics, USA) after the samples were degassed in vacuum at 120˚C overnight. The zeta potential of catalysts in KNO_3 (10^{-3} M) solution were measured with a Malvern Zata-sizer (Model ZEN 2010, Malvern Instrument Co., UK) with ten consistent readings.

2.3. Evaluation of the Adsorption Capability

For the adsorption capability measurements, fresh dye solutions of methyl orange (MO), acid orange II (AOII) and methyl blue (MB) with concentration of 200 $mg{\cdot}L^{-1}$ were prepared, respectively. 100 mg photocatalyst sample was put into 50 mL the above dye solutions. The suspensions were sonicated (40 KHz, 150 W) for 15 min and stirred for 1 h at room temperature in dark to achieve absorption equilibrium. After separation through centrifugation at 12000 rpm, the remaining dye in solution was measured by UV-Vis spectrometer after 10 times dilution. Adsorption kinetics of the samples was carried out for 2 h and the process was similar to the below photocatalytic reaction process without light irradiation.

2.4. Photocatalytic Reaction

In the experiment of photocatalytic degradation, methyl orange (MO) was adopted as a typical organic pollutant. The light source was a 500 W Xe-arc lamp (Nanjing Xujiang Machine-electronic Plant) equipped with wavelength cutoff filters (1 M sodium nitrite solution, $\lambda \geq 400$ nm) used as visible light source [30]. At each time, 100 mg of the powdered photocatalyst was added into a 200 mL solution of MO dye (20 $mg{\cdot}L^{-1}$) in a Pyrex-glass cell at room temperature and sonicated for 15 min to make the powders disperse well in the solution. Then the suspension system was magnetically stirred in the dark for 60 min to achieve adsorption/desorption equilibrium. After that, the concentration of the MO was adjusted to the same (15 $mg{\cdot}L^{-1}$), and then the solution was bubbled with air and irradiated with the visible-light. At regular intervals, an 8 mL of suspension was sampled and sepa-

rated by centrifugation at 12,000 rpm for 10 min. The concentration of the remaining MO was measured by its absorbance (A) at 465 nm with a Hitachi UV-3010 spectrophotometer. The degradation ratio of MO was calculated by $X = (A_0 - A)/A_0 \times 100\%$.

3. Results and Discussion

3.1. Morphology and Structures of the Samples

Figure 1 displays the XRD patterns of the prepared AgCl, CeO_2, AgCl/CeO_2 and Ag-AgCl/CeO_2 samples. **Figures 1(a)** and **(b)** exhibit the characteristic diffraction peaks of AgCl (JCPDS file No. 31-1238) and CeO_2 (JCPDS file No. 43-1002), respectively. Compared with **Figure 1(b)**, additional peaks appear in **Figure 1(c)**, which can be attributed to the cubic phase of AgCl, indicating that a crystalline cubic phase AgCl was formed on CeO_2. After irradiation with mercury lamp, the diffraction peak of metallic Ag (JCPDS file No. 65-2871) appears in Figure 1d due to the photo-reduction of some Ag^+ in AgCl to Ag^0. The reduced Ag atoms aggregate to form small silver nanocrystals with the cubic phase of Ag (111) located at 38.1˚, corresponding to 2.36 Å of lattice space, and then deposit on the surface of AgCl particles.

Figure 2 shows the SEM, TEM and EDS results of the prepared Ag-AgCl/CeO_2. According to **Figure 2 (a)** and **(b)**, CeO_2 presents a porous structure and Ag/AgCl NPs disperse well on the surface of CeO_2 with diameter in the range of 10 - 30 nm. To demonstrate the formation of silver nanoparticles on silver chloride nanoparticles,

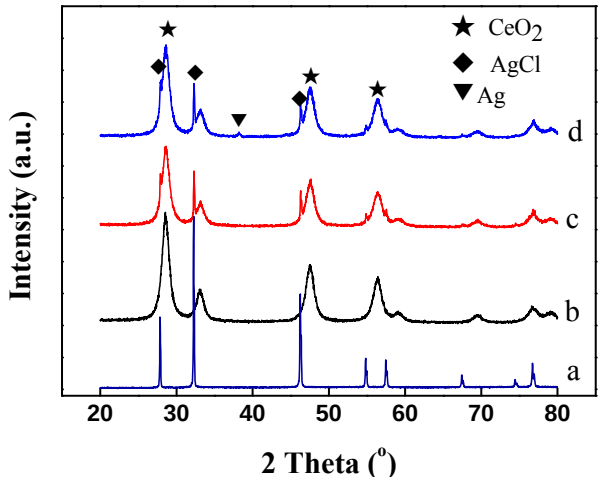

Figure 1. XRD patterns of AgCl (a); CeO_2 (b); AgCl/CeO_2 (c); and Ag-AgCl/CeO_2 (d).

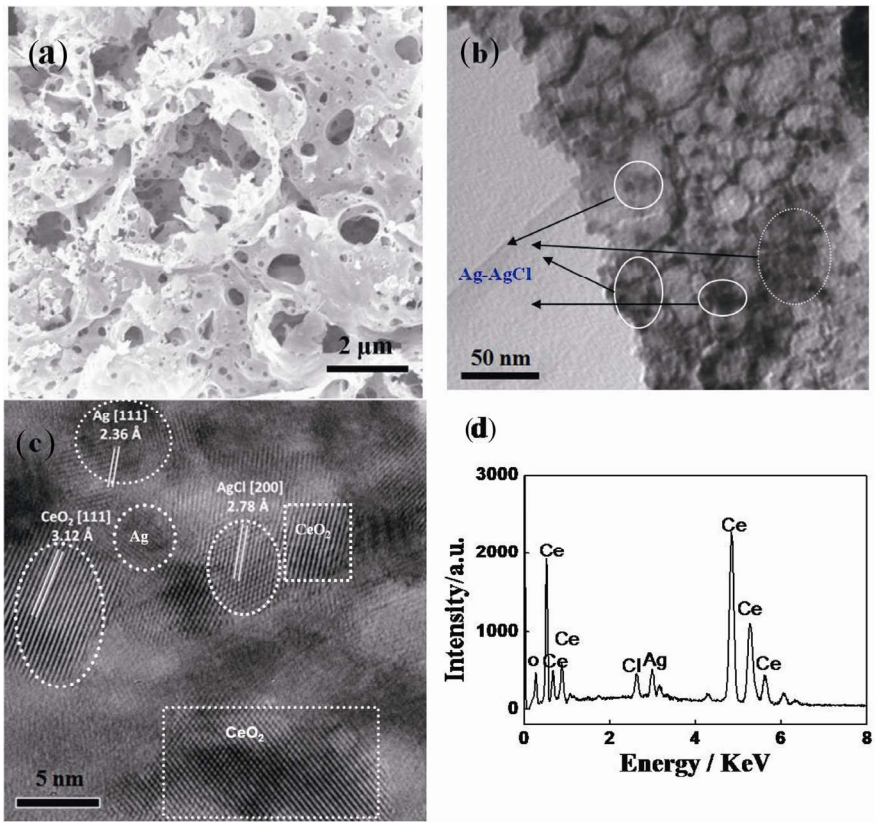

Figure 2. SEM (a) and TEM; (b) and HRTEM; (c) Images and EDS; (d) Pattern of Ag-AgCl/CeO_2.

high resolution-TEM analysis was shown in **Figure 2(c)**. Some lattice stripes with different orienttations could be observed clearly in **Figure 2(c)**. The characteristic values of lattice constant are 2.36, 2.78 and 3.12 Å corresponding to Ag (111), AgCl (200) and CeO_2 (111), respectively, which are coincident with the strong diffraction peaks of Ag, AgCl and CeO_2 from XRD results. The energy dispersive X-ray spectroscopy (EDS), as shown in **Figure 2(d)**, also confirmed the existence of Ce, O, Ag and Cl in Ag-AgCl/CeO_2, and the atomic percentages (%) of Ag and Cl in Ag/AgCl/CeO_2 sample is about 0.68 and 0.41. The atomic radio of Ag: Cl > 1, which further confirmed that the process of Ag^+ reducetion to Ag^0 happened and some Ag^0 existed in the form of metallic Ag.

The chemical status of Ag from AgCl/CeO_2 and Ag-AgCl/CeO_2 were further analyzed by XPS, as shown in **Figure 3**. Before irradiation, the Ag $3d_{5/2}$ and Ag $3d_{3/2}$ appear at the binding energies of 373.6 eV and 367.6 eV, respectively. After irradiation, the corresponding peaks shift to the binding energies of 373.3 eV and 367.3 eV, respectively. The difference of Ag 3d binding energy between AgCl/CeO_2 and Ag-AgCl/CeO_2 is attributed to the metallic Ag in the Ag-AgCl/CeO_2 [31].

The UV-Vis diffuse-reflectance spectra of CeO_2, AgCl/CeO_2 and Ag-AgCl/CeO_2 were compared in **Figure 4**. The CeO_2 (**Figure 4 (a)**) only exhibits a weak absorption in the visible light region around 400 nm - 450 nm.

The addition of AgCl doesn't enhance the absorption of CeO_2 due to the large band gaps of AgCl with a direct band gap of 5.15 eV (241 nm) and an indirect band gap of 3.25 eV (382 nm) [32] (**Figure 4(b)**). In contrast to AgCl/CeO_2 and CeO_2, Ag-AgCl/CeO_2 has a strong adsorption in the visible region of 400 - 700 nm (**Figure 4(c)**), which is attributed to the plasmonic resonance of Ag NPs deposited on AgCl/CeO_2 particles. It also further confirmed the formation of Ag NPs in the as-synthesized Ag-AgCl/CeO_2 catalyst.

On the basis of the above XRD, EDS, XPS, UV-Vis, SEM and TEM analysis, it can be confirmed that Ag-AgCl NPs deposited uniformly on the surface of CeO_2 and that some Ag^+ in AgCl was reduced to Ag^0 and thus Ag^0 and AgCl coexist in the Ag-AgCl/CeO_2 catalyst.

3.2. The Adsorption Behaviors of Samples

Figure 5 shows the adsorption kinetics of the catalysts to MO. After 30 min, all of the catalysts almost reach adsorption equilibrium. After 2 hours, about 29% of MO was adsorbed onto Ag-AgCl/CeO_2. Under the same condition, about 83%, 63% and 33% of MO were adsorbed onto AgCl/CeO_2, Ag/CeO_2 and CeO_2, respectively. AgCl/CeO_2 shows the strongest adsorption capability to MO.

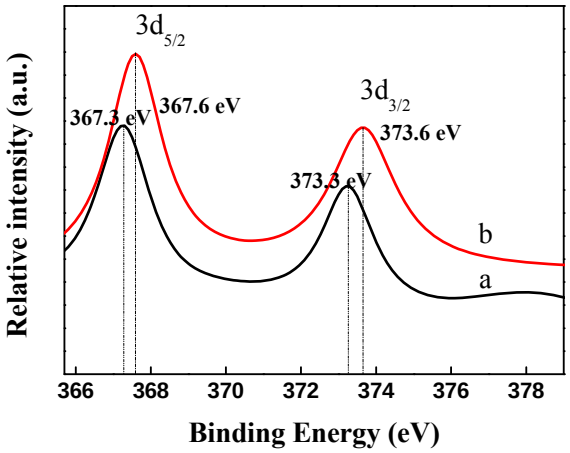

Figure 3. XPS spectra of Ag 3d of Ag-AgCl/CeO_2 (a) and AgCl/CeO_2 (b).

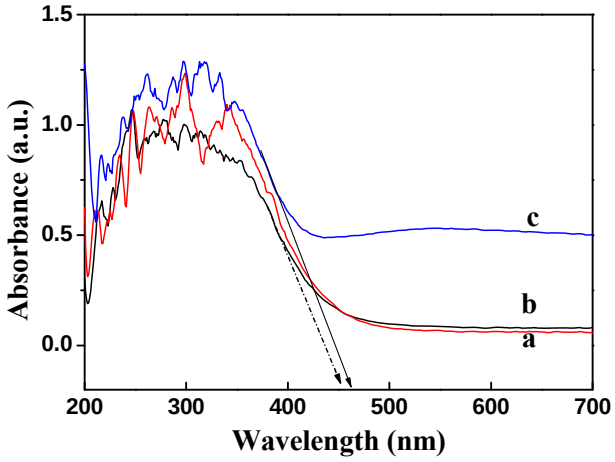

Figure 4. UV-Vis diffuse-reflectance spectra of CeO_2 (a); AgCl/CeO_2 (b) and Ag-AgCl/CeO_2 (c).

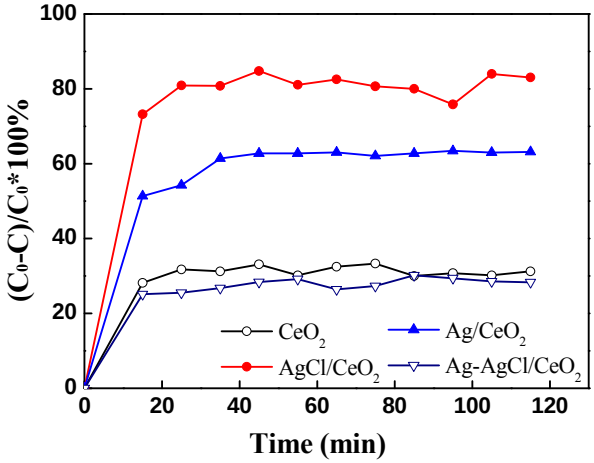

Figure 5. Adsorption kinetics of MO on the catalysts in dark.

The adsorption of these catalysts to MO and other organic dyes, such as MB and AOII were listed in **Table 1**. From **Table 1**, it can be concluded that all of the catalysts show higher absorption capability to anionic dyes, *i.e.*, MO and AOII. But they are inactive to cationic dye MB. It is interesting that $AgCl/CeO_2$ has the strongest adsorption ability to both MO and AOII among the three catalysts, although they have almost the same BET surface areas (**Table 1**). From the Zeta potential listed in **Table 1**, it can be seen that $AgCl/CeO_2$ has the highest zeta potential among the three catalysts, which means that the catalyst with more positive zeta potential owns the stronger adsorption capability to the anionic charged dyes. From these results, it is reasonable to conclude that the adsorption of the catalysts to dyes is due to the strong electrostatic interaction between anionic dyes and positively charged surfaces of the catalysts.

3.3. Photocatalytic Performances of Samples

The photocatalytic activity of the catalysts was evaluated by photocatalytic degradation of MO aqueous solution under visible light irradiation. In order to avoid the effects of the adsorption on the photodegradation efficiency, the initial concentration of the MO was adjust to the same level (15 $mg \cdot L^{-1}$) after the adsorption equilibrium. Figure 6 shows the degradation ratios of MO dye over different catalysts under visible light irradiation. It can be seen that the CeO_2 shows rather poor photocatalytic activity (**Figure 6 (a)**) with less than 5% of MO degradation ratio under visible light irradiation in 120 min. For Ag/CeO_2 sample with only Ag immobilized on CeO_2, it shows almost the same poor activity as that of CeO_2 (**Figure 6(b)**). For $AgCl/CeO_2$, almost 16% of MO could be degraded under the same condition (**Figure 6(d)**). The enhanced photocatalytic activity of $AgCl/CeO_2$ could be attributed to the synergy between the photosensitive AgCl and CeO_2. Under visible-light irradiation, the photogenerated electron-hole pairs were formed on the surface of CeO_2. The photoexcited electrons were separated into two parts: One part of them were scavenged by oxygen on the catalyst surface to produce O_2^- active species, the other part transferred to AgCl to reduce a small amount of Ag^+ to Ag^0 depositing on the surface of AgCl NPs. From Figure 6d, it can also be seen that the degradation ratio of MO on $AgCl/CeO_2$ becomes distinct after 40 min because of the formation of Ag NPs on the surface of $AgCl/CeO_2$ surface. For $Ag\text{-}AgCl/CeO_2$, the degradation ratio of MO reaches 90% in 120 min (**Figure 6(e)**), which is more than 5 and 16 times those of $AgCl/CeO_2$ and Ag/CeO_2, respectively. It is proven that Ag NPs with surface plasmon resonance dramatically enhanced the photocatalytic activity under the visible-light irradiation. In order to estimate the role of CeO_2, the photocatalytic degradation of MO with Ag-AgCl sample with same Ag/AgCl content as $Ag\text{-}AgCl/CeO_2$ were shown in **Figure 6(c)**. It can be seen that Ag-AgCl catalyst shows lower activity with less than 10% MO being degraded. All the results above suggest that Ag, AgCl and CeO_2 in the $Ag\text{-}AgCl/CeO_2$ catalyst exhibited synergistic effects.

In order to investigate the role of Ag in the $Ag\text{-}AgCl/CeO_2$ further, the photodegradation of MO with $Ag\text{-}AgCl/CeO_2$ and $AgCl/CeO_2$ were studied under different visible-light, respectively, as shown in **Figure 7**. The visible-light with different wavelength was obtained with different filter. From **Figure 7(d)**, at the wavelength $\lambda > 420$ nm, no significant degradation was observed on $AgCl/CeO_2$, which is due to the weak visible-light absorption of $AgCl/CeO_2$ in this wavelength range. While $Ag\text{-}AgCl/CeO_2$ exhibited very high photocatalytic activity at the same condition, which means that Ag plays very important role in the photocatalytic degradation of MO. One is the plasmon resonance of Ag NPs and the other is the enhancing separation of photo-excited electrons and holes. With wavelength changing from $\lambda > 400$ nm to $\lambda > 420$

Table 1. Adsorption capacity and zeta potential of different catalysts

Catalysts	Adsorption Capacity ($\mu mol \cdot g^{-1}$)			Zeta potential (mV)	BET surface area ($m^2 \cdot g^{-1}$)
	MO	MB	AOII		
$AgCl/CeO_2$	209.8	0	185.9	26.4	51.2
Ag/CeO_2	125.3	0	164.5	21.8	53.3
$Ag\text{-}AgCl/CeO_2$	77.3	0	73.71	20.5	56.4

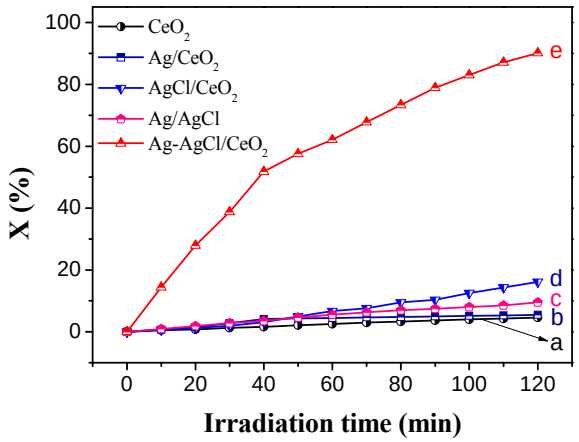

Figure 6. The degradation ratios of MO under visible light irradiation on the catalysts: CeO_2 (a); Ag/CeO_2 (b); Ag-AgCl (c); $AgCl/CeO_2$ (d); and $Ag\text{-}AgCl/CeO_2$ (e).

nm, the photocatalytic activity of Ag-AgCl/CeO_2 changes little and the change is even smaller than that for AgCl/CeO_2, which indicates that the plasmon resonance of Ag NPs is the main role in the photocatalytic degradation of MO under visible-light [28].

The effect of photo-reduction time of AgCl/CeO_2 on the photocatalytic degradation of MO was also examined. The result showed that Ag-AgCl/CeO_2 with photo-reduction time of 20 min exhibits the highest photocatalytic activity than those with reduction time of 10 min and 30 min, indicating that the photocatalytic activity greatly depends on the Ag NPs content on AgCl/CeO_2.

As a useful photocatalyst, the stability is rather important for its practical application. **Figure 8** shows the reusability of Ag-AgCl/CeO_2 catalyst for MO photocatalytic degradation. Although the degradation ratio of MO decreased slightly after each run, the catalyst still exhibited efficient activity with about 82% of the degradation ratio at the fifth run. So, the as-prepared catalyst could remain 90% of the initial activity after five recycling run, suggesting the Ag-AgCl/CeO_2 has good stability and can be used repeatedly.

3.4. Discussion on the Reaction Mechanism

Several studies have confirmed that Ce 4f plays vital role for CeO_2 in photocatalytic process [33] and they demonstrated that electrons can be more easily injected into 4f band of CeO_2 because the potential of 4f band of CeO_2 is a little more positive than that of the conduction band of TiO_2. CeO_2 was chosen as the semiconductor in this work has other reason, that is, CeO_2 has excellent electron-transfer mediator ability under visible light [9], which is helpful to further enhance its charge separation ability.

For a plasmonic photocatalyst, the major photocatalytic reaction procedure under visible light irradiation can be summarized by the following steps, schematically shown in **Figure 9**, which is similar with Huang's mechanism of Ag@AgCl plasmonic photocatalysis and Hu's plasmon-induced charge separation mechanism [22,27]. First, due to the SPR ability of noble metal NPs, Ag NPs absorb visible light and generate electron-hole pairs when the visible light is illuminated. Then the photogenerated electrons are injected to the 4f band of CeO_2 and captured by the oxygen on the surface of CeO_2 to generate superoxide radical that can then form hydrogen peroxide (H_2O_2), hydroperoxy ($HO_2\cdot$) and hydroxyl ($OH\cdot$). Except for the generation of these common photocatalytic active species, another reactive radical species Cl^0 is formed when the holes transfer to AgCl with its surface negatively charged by Cl^- after Ag^+ reduction. Cl^0 can oxidize MO and be reduced to Cl^- again. So, the system is cyclic and stable.

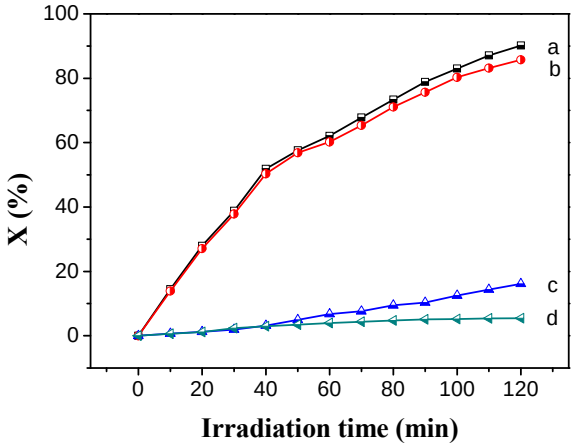

Figure 7. The degradation ratios of MO dye in solution (20 mg·L^{-1}) under visible light with $\lambda \geq 400$ nm (a, c) and $\lambda \geq 420$ nm (b, d) on the catalysts: Ag-AgCl/CeO_2 (a, b) and AgCl/CeO_2 (c, d).

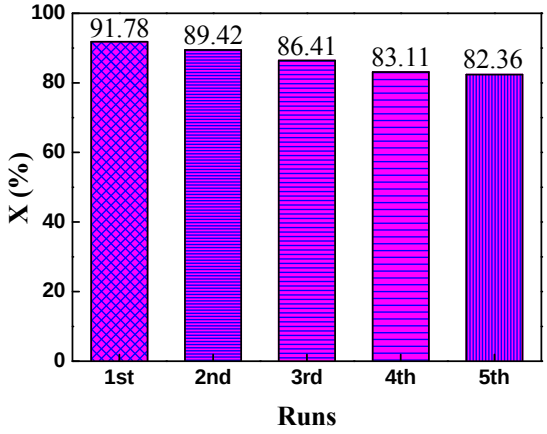

Figure 8. Reusability of Ag-AgCl/CeO_2 catalyst for MO photocatalytic degradation under visible light irradiation. MO initial concentration of 15 mg·L^{-1}; catalyst concentration of 0.5 g·L^{-1} and reaction time of 2 h.

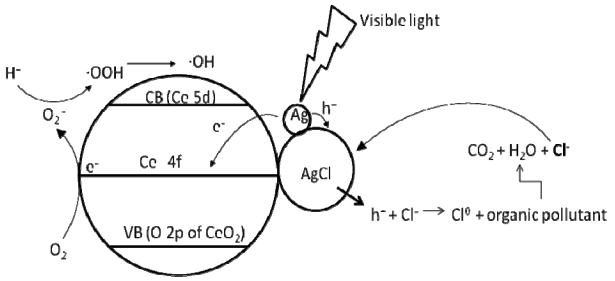

Figure 9. Schematic diagram for the charge separation on Ag-AgCl/CeO_2 catalyst under visible light irradiation.

4. Conclusions

The plasmonic photocatalyst Ag-AgCl/CeO_2 was prepared with an easy achieving and controlling method.

The results show that Ag-AgCl/CeO_2 has high photocatalytic activity and good stability for MO photocatalytic degradation under visible light irradiation. With the synergistic effects of Ag and AgCl, an improved visible-light photocatalytic activity was achieved. Ag-AgCl/CeO_2 will be a potentially promising plasmonic photocatalysts for organic pollutant degradation and water purifycation.

5. Acknowledgements

The authors thank the National Natural Science Foundation of China (No. 20873044) and the Guangdong Provincial Science and Technology Project of China (No. 2011B050400014).

6. References

[1] A. Fujishima and K. Honda, "Electrochemical Photocatalysis of Water at a Semiconductor Electrode," *Nature*, Vol. 238, No. 5358, 1972, pp. 37-38.

[2] B. Ohtani, R. M. Bowman, D. P. Colombo, H. Kominami, H. Noguchi and K. Uosaki, "Femtosecond Diffuse Reflectance Spectroscopy of Aqueous Titanium(IV) Oxide Suspension: Correlation of Electron-Hole Recombination Kinetics with Photocatalytic Activity," *Chemistry Letters*, Vol. 27, No. 7, 1998, pp. 579-580. doi:10.1246/cl.1998.579

[3] S. Ikeda, N. Sugiyama, B. Pal, G. Marci, L. Palmisano, H. Noguchi, *et al*., "Photocatalytic Activity of Transition-Metal-Loaded Titanium(IV) Oxide Powders Suspended in Aqueous Solutions: Correlation with Electron-Hole Recombination Kinetics," *Physical Chemistry Chemistry Physics*, Vol. 3, No. 2, 2001, pp. 267-273. doi:10.1039/b008028o

[4] A. Fujishima, X. T. Zhang and D. A. Tryk, "TiO_2 Photocatalysis and Related Surface Phenomena," *Surface Science Reports*, Vol. 63, No. 12, 2008, pp. 515-582. doi:10.1016/j.surfrep.2008.10.001

[5] T. W. Kim, S. J. Hwang, S. H. Jhung, J. S. Chang, H. Park, W. Choi, *et al*., "Bifunctional Heterogeneous Catalysts for Selective Epoxidation and Visible Light Driven Photolysis: Nickel Oxide-Containing Porous Nanocomposite," Advanced Materials, Vol. 20, No. 3, 2008, pp. 539-542. doi:10.1002/adma.200701677

[6] J. Li, W. H. Ma, Y. P. Huang, X. Tao, J. C. Zhao and Y. M. Xu, "Oxidative Degradation of Organic Pollutants Utilizing Molecular Oxygen and Visible Light over a Supported Catalyst of $Fe(bpy)_3^{2+}$ in Water," *Applied Catalysis B*: *Environmental*, Vol. 48, No. 1, 2004, pp. 17-24. doi:10.1016/j.apcatb.2003.09.003

[7] J. C. Zhao, C. C. Chen and W. H. Ma, "Photocatalytic Degradation of Organic Pollutants under Visible Light Irradiation," *Topics in Catalysis*, Vol. 35, No. 3-4, 2005, pp. 269-278. doi:10.1007/s11244-005-3834-0

[8] M. D. Hernandez-Alonso, F. Fresno, S. Suarez and J. M. Coronado, "Development of Alternative Photocatalysts to TiO_2: Challenges and Opportunities," *Energy & Environmental Science*, Vol. 2, No. 12, 2009, pp. 1231-1257. doi:10.1039/b907933e

[9] P. F. Ji, J. L. Zhang, F. Chen and M. Anpo, "Study of Adsorption and Degradation of Acid Orange 7 on the Surface of CeO_2 under Visible Light Irradiation," *Applied Catalysis B*: *Environmental*, Vol. 85, No. 3-4, 2009, pp. 148-154. doi:10.1016/j.apcatb.2008.07.004

[10] G. R. Bamwenda, K. Sayama and H. Arakawa, "The Photoproduction of O_2 from a Suspension Containing CeO_2 and Ce^{4+} Cations as an Electron Acceptor," *Chemistry Letters*, Vol. 28, No. 10, 1999, pp. 1047-1048. doi:10.1246/cl.1999.1047

[11] Q. Fu, H. Saltsburg and M. Flytzani-Stephanopoulos, "Active Nonmetallic Au and Pt Species on Ceria Based Water Gas Shift Catalysts," *Science*, Vol. 301, No. 5635, 2003, pp. 935-938. doi:10.1126/science.1085721

[12] E. Perry Murray, T. Tsai and S. A. Barnett, "A Direct-Methane Fuel Cell with Ceria-Based Anode," *Nature*, Vol. 400, No. 6745, 1999, pp. 649-651. doi:10.1038/23220

[13] A. Corma, P. Atienzar, H. Garcia and J. Y. Chane-Ching, "Hierarchically Mesostructured Doped CeO_2 with Potential for Solar-Cell Use," *Nature Materials*, Vol. 3, No. 6, 2004, pp. 394-397. doi:10.1038/nmat1129

[14] V. Subramanian, E. Wolf and P. V. Kamat, "Semiconductor-Metal Composite Nanostructures. To What Extent Do Metal Nanoparticles Improve the Photocatalytic Activity of TiO_2 Films," *Journal of Physical Chemistry B*, Vol. 105, No. 46, 2001, pp. 11439-11446. doi:10.1021/jp011118k

[15] M. Miyauchi, A. Nakajima, T. Watanabe and K. Hashimoto, "Photocatalysis and Photoinduced Hydrophilicity of Various Metal Oxide Thin Films," *Chemistry of Materials*, Vol. 14, No. 6, 2002, pp. 2812-2816. doi:10.1021/cm020076p

[16] L. B. Khalil, W. E. Mourad and M. W. Rophael, "Photocatalytic Reduction of Environmental Pollutant Cr(VI) over some Semiconductors under UV/Visible Light Illumination," *Applied Catalysis B*: *Environmental*, Vol. 17, No. 3, 1998, pp. 267-273. doi:10.1016/S0926-3373(98)00020-4

[17] J. G. Yu, G. P. Dai and B. B. Huang, "Fabrication and Characterization of Visible-Light-Driven Plasmonic Photocatalyst Ag/AgCl/TiO_2 TiO_2 Nanotube Arrays," *Journal of Physical Chemistry C*, Vol. 113, No. 37, 2009, pp. 16394-16401. doi:10.1021/jp905247j

[18] K. Awazu, M. Fujimaki, C. Rockstuhl, J. Tominaga, H. Murakami, Y. Ohki, *et al*., "A Plasmonic Photocatalyst Consisting of Silver Nanoparticles Embedded in Titanium Dioxide," *Jouranl of the American Chemical Society*, Vol. 130, No. 5, 2008, pp. 1676-1680. doi:10.1021/ja076503n

[19] X. Chen, H. Y. Zhu, J. C. Zhao, Z. T. Zheng and X. P. Gao, "Visible-Light-Driven Oxidation of Organic Contaminants in Air with Gold Nanoparticle Catalysts on Oxide Supports," *Angewandte Chemie* (*International Edition*), Vol. 47, No. 29, 2008, pp. 5353-5356. doi:10.1002/anie.200800602

[20] S. M. Sun, W. Z. Wang, L. Zhang, M. Shang and L. Wang, "Ag@C Core/Shell Nanocomposite as a Highly Efficient Plasmonic Photocatalyst," *Catalysis Communications*, Vol. 11, No. 4, 2009, pp. 290-293. doi:10.1016/j.catcom.2009.09.026

[21] S. Rodrigues, S. Uma, I. N. Martyanov and K. J. Klabunde,

"AgBr/Al-MCM-41 Visible-Light Photocatalyst for Gas-Phase Decomposition of CH_3CHO," *Journal of Catalysis*, Vol. 233, No.2, 2005, pp. 405-410. doi:10.1016/j.jcat.2005.05.011

[22] P. Wang, B. B. Huang, X. Y. Qin, X. Y. Zhang, Y. Dai, J. Y. Wei, *et al*., "Ag@AgCl: A Highly Efficient and Stable Photocatalyst Active under Visible Light," *Angewandte Chemie* (*International Edition*), Vol. 47, No. 41, 2008, pp. 7931-7933. doi:10.1002/anie.200802483

[23] P. Wang, B. B. Huang, X. Y. Zhang, X. Y. Qin, H. Jin, Y. Dai, *et al*., "Highly Efficient Visible-Light Plasmonic Photocatalyst Ag@AgBr," *Chemistry—A European Journal*, Vol. 15, No. 8, 2009, pp. 1821-1824. doi:10.1002/chem.200802327

[24] P. Wang, B. B. Huang, Q. Q. Zhang, X. Y. Zhang, X. Y. Qin, Y. Dai, *et al*, "Highly Efficient Visible Light Plasmonic Photocatalyst Ag@Ag(Br,I)," *Chemistry—A European Journal*, Vol. 16, No. 33, 2010, pp. 10042-10047. doi: 10.1002/chem.200903361

[25] P. Wang, B. B. Huang, Z. Z. Lou, X. Y. Zhang, X. Y. Qin, Y. Dai, *et al*, "Synthesis of Highly Efficient Ag@AgCl Plasmonic Photocatalysts with Various Structures," *Chemistry—A European Journal*, Vol. 16, No. 2, 2010, pp. 538-544. doi:10.1002/chem.200901954

[26] Y. Tian and T. Tatsuma, "Mechanisms and Applications of Plasmon-Induced Charge Separation at TiO_2 Films Loaded with Gold Nanoparticles," *Jouranl of the American Chemical Society*, Vol. 127, No. 20, 2005, pp. 7632-7637. doi:10.1021/ja042192u

[27] X. F. Zhou, C. Hu, X. X. Hu, T. W. Peng and J. H. Qu, "Plasmon-Assisted Degradation of Toxic Pollutants with Ag-AgBr/Al_2O_3 under Visible-Light Irradiation," *Journal of Physical Chemistry C*, Vol. 114, No. 6, 2010, pp. 2746-2750. doi:10.1021/jp909697k

[28] C. Hu, T. W. Peng, X. X. Hu, Y. L. Nie, X. F. Zhou, J. H. Qu, et al, "Plasmon-Induced Photodegradation of Toxic Pollutants with Ag-AgI/Al_2O_3 under Visible-Light Irradiation," *Jouranl of the American Chemical Society*, Vol. 132, No. 2, 2010, pp. 857-862. doi:10.1021/ja907792d

[29] C. Hu, Y. Q. Lan, J. H. Qu, X. X. Hu and A. M. Wang, "Ag/AgBr/TiO_2 Visible Light Photocatalyst for Destruction of Azodyes and Bacteria," *Journal of Physical Chemistry B*, Vol. 110, No. 9, 2006, pp. 4066-4072. doi:10.1021/jp0564400

[30] C. Ping, L. Wei, T. L. Zhou, Y. P. Jin and M. Y. Gu, "Physical and Photocatalytic Properties of Zinc Ferrite Doped Titania under Visible Light Irradiation," *Journal of Photochemistry and Photobiology A*: *Chemistry*, Vol. 168, No. 1-2, 2004, pp. 97-101. doi:10.1016/j.jphotochem.2004.05.018

[31] J. F. Hamilton, "Physical Properties of Silver Halide Microcrystals," *Photographic Science and Engineering*, Vol. 18, No. 5, 1974, pp. 493-500.

[32] S. Glaus and G. Calzaferri, "The Band Structures of the Silver Halides AgF, AgCl, and AgBr: a Comparative Study," P*hotochemical & Photobiological Sciences*, Vol. 2, No. 4, 2003, pp. 398-401. doi:10.1039/b211678b

[33] F. B. Li, X. Z. Li, M. F. Hou, K. W. Cheah and W. C. H. Choy, "Enhanced Photocatalytic Activity of Ce^{3+}-TiO_2 for 2-Mercaptobenzothiazole Degradation in Aqueous Suspension for Odour Control," A*pplied Catalysis A*: *General*, Vol. 285, No. 1-2, 2005, pp. 181-189. doi:10.1016/j.apcata.2005.02.025

